We are IntechOpen, the world's leading publisher of Open Access books Built by scientists, for scientists

4,800
Open access books available

122,000
International authors and editors

135M
Downloads

Our authors are among the

154
Countries delivered to

TOP 1%
most cited scientists

12.2%
Contributors from top 500 universities

CLARIVATE ANALYTICS BOOK CITATION INDEX INDEXED

WEB OF SCIENCE™

Selection of our books indexed in the Book Citation Index in Web of Science™ Core Collection (BKCI)

Interested in publishing with us?
Contact book.department@intechopen.com

Numbers displayed above are based on latest data collected.
For more information visit www.intechopen.com

27

Sub-Wavelength Patterning of Self-Assembled Organic Monolayers via Nonlinear Processing with Femtosecond Laser Pulses

Nils Hartmann
Center for Nanointegration Duisburg-Essen (CeNIDE)
Universität Duisburg-Essen
Germany

1. Introduction

Self-assembled monolayers (SAMs) are ultrathin organic coatings, which allow one to precisely tailor surface properties, such as the wettability, the biocompatibility and the chemical reactivity and resistance. For this reason, SAMs are widely used as ultrathin resists and functional coatings in numerous micro- and nanofabrication schemes (Love et al., 2005; Onclin et al, 2005; Buriak, 2002). Femtosecond (fs) laser processing of SAMs here offers a variety of particularly promising perspectives (Hartmann et al., 2008; Franzka et al., 2010; Mathieu et al., 2010). On one hand, fs-laser processing is a maskless noncontact technique with a high flexibility, both, in two and three dimensions. Also, processing can be carried out at high pressures, in liquids and on - or even in - dielectric materials and rapid patterning is feasible over wafer scale areas. In addition, fs-lasers allow for nonlinear processing and hence provide a means for sub-wavelength patterning. On the other hand, because of their ultrathin nature, SAMs can be processed with single laser pulses, which ensures short processing times. The monomolecular thickness also allows for well-defined irradiation and burr-free patterning of the coating and avoids bubble and particle formation. All off which are problems commonly encountered in direct ablative fs-laser processing. Moreover, varying the chemical structure of the monolayer provides a means to tailor cross sections, incubation effects and resist properties and to enable chemical patterning. Surprisingly, though, despite these promising perspectives, fs-laser processing of organic monolayers still is largely unexplored (Chang et al., 2005; Chang et al., 2006; Kirkwood et al., 2007; Álvarez et al., 2008). Moreover, most of these contributions focus on micropatterning experiments (Chang et al., 2006; Kirkwood et al., 2007; Álvarez et al., 2008). This chapter reviews recent efforts in sub-wavelength patterning of organic monolayers via single pulse fs-laser processing including silane-based monolayers on quartz glass (Hartmann et al., 2008) and surface-oxidized silicon substrates (Franzka et al., 2010) and thiol-based monolayers on gold-coated silicon substrates (Mathieu et al., 2010). These results demonstrate the general versatility of fs-lasers in nonlinear processing of SAMs on dielectric, semiconducting and metallic platforms and emphasize the particular prospects of this approach as a tool for rapid micro- and nanofabrication.

2. Self-assembled monolayers

Fig. 1 displays the general structure of SAMs (Mathieu & Hartmann, 2010). Generally, these ultrathin films consist of densely packed elongated molecules, which stand up on top of the substrate's surface. The film thickness typically is 1-2 nm. Each molecule can be divided into three functional parts: i) the head group, which couples the molecules to the surface and defines the type of the SAM. Most prominent are thiol-based SAMs on gold and other coinage metals (Love et al., 2005), silane-based SAMs on oxidic or surface-oxidized substrates (Onclin et al., 2005) and organic monolayers from olefinic precursor molecules on semiconducting platforms (Buriak, 2002). ii) the backbone, which in the simplest case represents an aliphatic hydrocarbon chain, and iii) the end group, e. g. simple functional groups such as amine or carboxyl groups or more complex chemical or biochemical functionalities. Upon varying the chemical structure the chemical reactivity and resistance of SAMs can be tailored. This explains the wide-spread use of SAMs as ultrathin resists and functional coatings (Love et al., 2005; Onclin et al., 2005; Buriak, 2002). In particular, via the end group additional components can be attached to the surface. In conjunction with patterning routines this provides a facile means to fabricate chemical templates with domains of defined size, shape and chemical termination. Such platforms allow one to selectively couple nanoscopic building blocks in predefined surface areas in order to build up functional surface architectures (Woodson & Liu, 2007).

A common procedure for the preparation of SAMs considers immersion of clean substrates into millimolar solutions of respective precursor molecules. With time the molecules couple to the substrate surface via the head group, stand up on the surface and form a densely packed monolayer as depicted in Fig. 1. Monolayer growth is self-limiting, as the end groups usually are chosen as to not react with the head groups. The quality of the monolayer in terms of packing density and order, however, strongly depends on the type of the SAM and the detailed preparation conditions (Love et al., 2005; Onclin et al., 2005; Buriak, 2002).

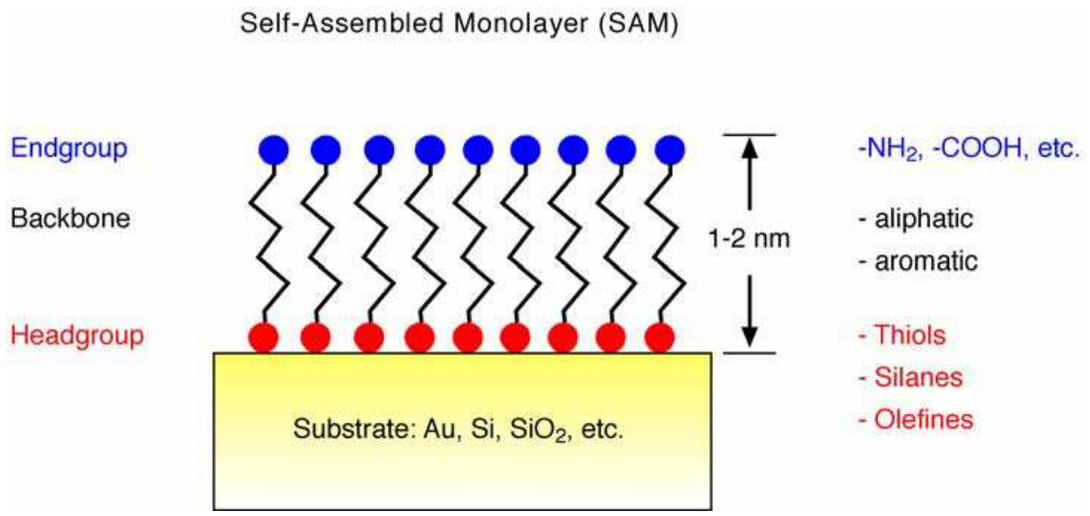

Fig. 1. Schematic diagram of the structure of SAMs. The thickness typically is 1-2 nm. Three functional parts of the adsorbed molecules are distinguished: the head group, the backbone and the end group. Adapted from Mathieu & Hartmann, 2010. © IOP.

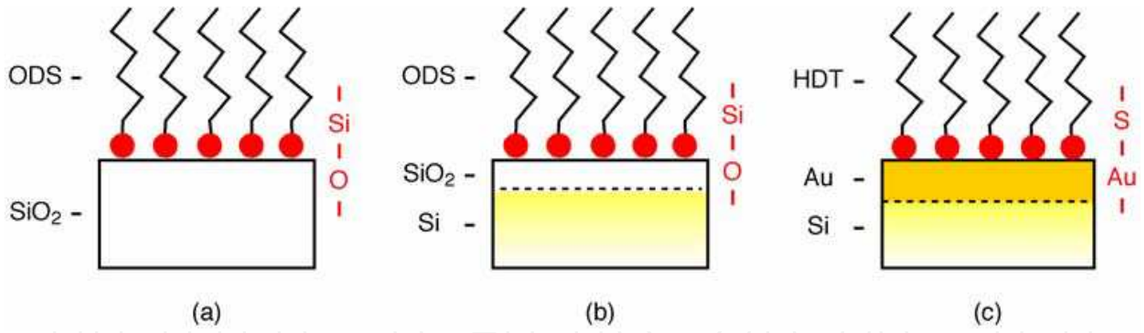

Fig. 2. Schematic presentations of the SAM/substrate combinations considered in this review: a) ODS monolayers on quartz glass, b) ODS monolayers on surface-oxidized silicon substrates, c) HDT monolayers on Au-coated silicon substrates. The surface bond of the molecules is shown in red on the right-hand side of each scheme.

In the work reviewed here, alkylsiloxane SAMs and alkanethiol SAMs are addressed. As substrates quartz glass, surface-oxidized silicon and Au-coated silicon samples are used. Surface-oxidized silicon samples expose a native oxide layer with a thickness of 1-2 nm on top. Au-coated silicon samples are silicon samples with a 5 nm Ti adhesion layer and a 40 nm Au layer on top. Detailed coating procedures are given in the literature (Hartmann et al., 2008; Franzka et al., 2010; Mathieu et al., 2010). Briefly, prior to coating, all substrates are cleaned in hot piranha solution (a mixture of sulfuric acid and hydrogen peroxide). Octadecylsiloxane (ODS) monolayers then are formed upon immersion of the substrates into a millimolar solution of octadecyltrichlorosilane in toluene. For coating with hexadecanthiol (HDT) monolayers a millimolar solution of HDT in ethanol is used. Schematic presentations of the distinct SAM/substrate combinations are shown in Fig. 2.

3. Nonlinear femtosecond laser processing

Laser processing is widely recognized as a facile and versatile means for direct patterning of SAMs (Mathieu & Hartmann, 2010). If nanopatterning is targeted, the optical diffraction limit, however, poses a significant constraint (Bäuerle, 2000). Even if highly focusing optics with a numerical aperture NA close to one is used the minimum structure size d_{min} usually is not much smaller than the wavelength λ of the laser light:

$$d_{\min} \approx \lambda / NA \tag{1}$$

A common means to extend the lateral resolution of laser techniques into the sub-wavelength range takes advantage of nonlinear effects (Bäuerle, 2000; Koch et al., 2005a; Ali et al., 2008; Chong et al., 2010). If one considers the complexity of photoexcited processes at surfaces, the pool of nonlinearities, of course, is large (Zhou et al., 1991; Richter & Cavanagh, 1992; Zimmermann & Ho, 1995; Mathieu & Hartmann, 2010). In general, direct and indirect excitation mechanisms can be distinguished. Direct mechanisms are based on an immediate excitation of the adsorbed molecules within the monolayer. Examples include photoexcitation via single or multiphoton processes and field-induced processes. In contrast, indirect mechanisms start with excitation processes that are initiated in the substrate. Absorption of laser light in the substrate at first generates excited charge carriers, such as hot electrons. On one hand, these electrons may interact with the adsorbed molecules

building up the monolayer and initiate reactions. Examples are photochemical or photoelectrochemical reaction pathways. On the other hand, the excited electrons eventually scatter inelastically with the substrate lattice, which inevitably results in a certain temperature rise at the surface. This provides the basis for photothermal reaction pathways.
All the aforementioned processes proceed on material-specific time, length and energy scales, which vary over several orders of magnitude. This makes laser patterning a rich and complex process (Bäuerle, 2000). For this reason, nonlinear laser processing of organic monolayers, at first, necessitates a proper choice of all laser parameters in order to trigger the desired surface reactions and avoid damage of the substrate (Mathieu & Hartmann, 2010). Fig. 3 depicts some of the essential energetic parameters: the photon energy E_P, the linear photodissociation threshold E_D of the monolayer and, if applicable, the band gap E_B of the substrate. Commonly, in nonlinear laser processing photon energies well below the photodissociation threshold are chosen. Femtosecond lasers here offer some particularly promising perspectives (Hartmann et al., 2008; Franzka et al., 2010; Mathieu et al., 2010). Processing of organic monolayers on dielectric materials with $E_B > E_P$ allows one to exploit multiphoton absorption processes. On semiconductors and metals with $E_B \leq E_P$, indirect processes, e. g. multiple electronic excitations or photothermal reactions can be initiated. All these processes introduce strong nonlinearities and ensure sub-wavelength resolution. Note, although fs-lasers commonly are used in order to minimize thermal impact, photothermal pathways could open up shortly after local irradiation with fs-laser pulses.

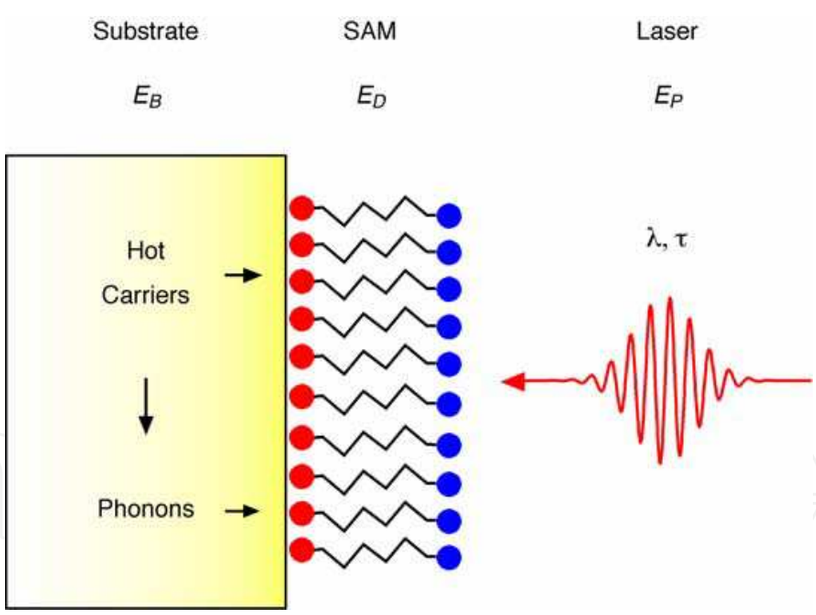

Fig. 3. Energetic constraints and photoexcited processes in fs-laser processing. Adapted from Mathieu & Hartmann, 2010. © IOP.

Laser processing experiments described in this work have been carried out at the Laser Zentrum Hannover (LZH) using a commercial Ti:Sapphire oscillator-amplifier system (Femtopower compact Pro, Femtolasers Produktions GmbH) at ambient conditions. A detailed description of the experimental setup is given in the literature (Koch et al., 2006). The laser system provides Gaussian laser pulses with a wavelength and a pulse length of $\lambda = 800$ nm and $\tau < 30$ fs, respectively. A Schwarzschild microscope objective with $NA = 0.5$

is used to focus the laser pulses onto the substrates. The 1/e focal spot diameter $d_{1/e}$ somewhat varies depending on the specific objective and the optical adjustment of the experimental setup. Respective values in each experiment are obtained upon fitting the experimental data as outlined below.
Typically, single-pulse processing at distinct pulse energies E is carried out. Fluences F are calculated via (Hartmann et al., 2008):

$$F = 4E/\pi d_{1/e}^2 \tag{2}$$

For characterization of the patterned samples atomic force microscopy (AFM) is used. AFM images are recorded in contact mode with standard cantilevers. The diameter d of the structures usually depends on the laser fluence as follows (Hartmann et al., 2008):

$$d = d_{1/e}\sqrt{\ln\left(F/F_{th}\right)} \tag{3}$$

where F_{th} is a critical threshold for a given process, e. g. for monolayer decomposition or substrate ablation. For analysis, the experimental data is fitted on the basis of Eq. (3). This yields the corresponding critical threshold value F_{th} and the 1/e spot diameter $d_{1/e}$.

3.1 Alkylsiloxane monolayers on quartz glass

Femtosecond laser patterning of alkylsiloxane monolayers on quartz glass at $\lambda = 800$ nm allows one to exploit multiphoton absorption processes (Hartmann et al., 2008). In particular, photochemical patterning of these coatings usually is carried out at $\lambda < 200$ nm (Sugimura et al., 2000). The linear photodissociation energy E_D is expected to be around 6 eV. Quartz glass, in turn, exhibits a band gap E_B of 9 eV. Hence, at a photon energy of $E_P = 1.6$ eV considered here, nonlinear processing appears feasible. Moreover, in view of these energetic constraints, it has been anticipated, that sub-wavelength patterning of the coating can be carried out well below the ablation threshold of the substrate.
Fig. 4 shows AFM data from experiments, in which coated samples are patterned with single laser pulses at distinct fluences. Local irradiation results in circular spots of varying morphology and size. At high laser fluences, two regions can be distinguished (Fig. 4a). In the inner region ablation of the substrate is evident. In particular, here, depths reach deep into the bulk (Fig. 4c). In contrast, depths in the outer region remain below 2 nm indicative for a decomposition of the organic monolayer. Note, the outer and the inner region can also be clearly distinguished in the friction contrast (Fig. 4b). In the following the diameters of these regions, where monolayer decomposition and substrate ablation are observed, are denoted as d_{SAM} and d_{quartz}, respectively (Fig. 4d).
At lower laser fluences, no substrate ablation is observed (Figs. 4e-h). Decomposition of the monolayer, however, takes place down to very low fluences. In Fig. 5a a plot of the diameters d_{SAM} and d_{quartz} over the full range of laser fluences considered here is displayed. A fit of the data on the basis of Eq. (3) yields critical threshold values for monolayer decomposition $F_{th}^{SAM} = 3.1$ J/cm² and substrate ablation $F_{th}^{quartz} = 4.2$ J/cm². This points to a fairly large parameter range for selective processing of the monolayers. Moreover, in this regime sub-wavelength patterning below $\lambda/3$ is possible. In particular, as shown in Fig. 5b, at $d_{1/e} = 1.8$ µm structures with a width of 250 nm and below are fabricated. Note, these structures also come with sharp edges.

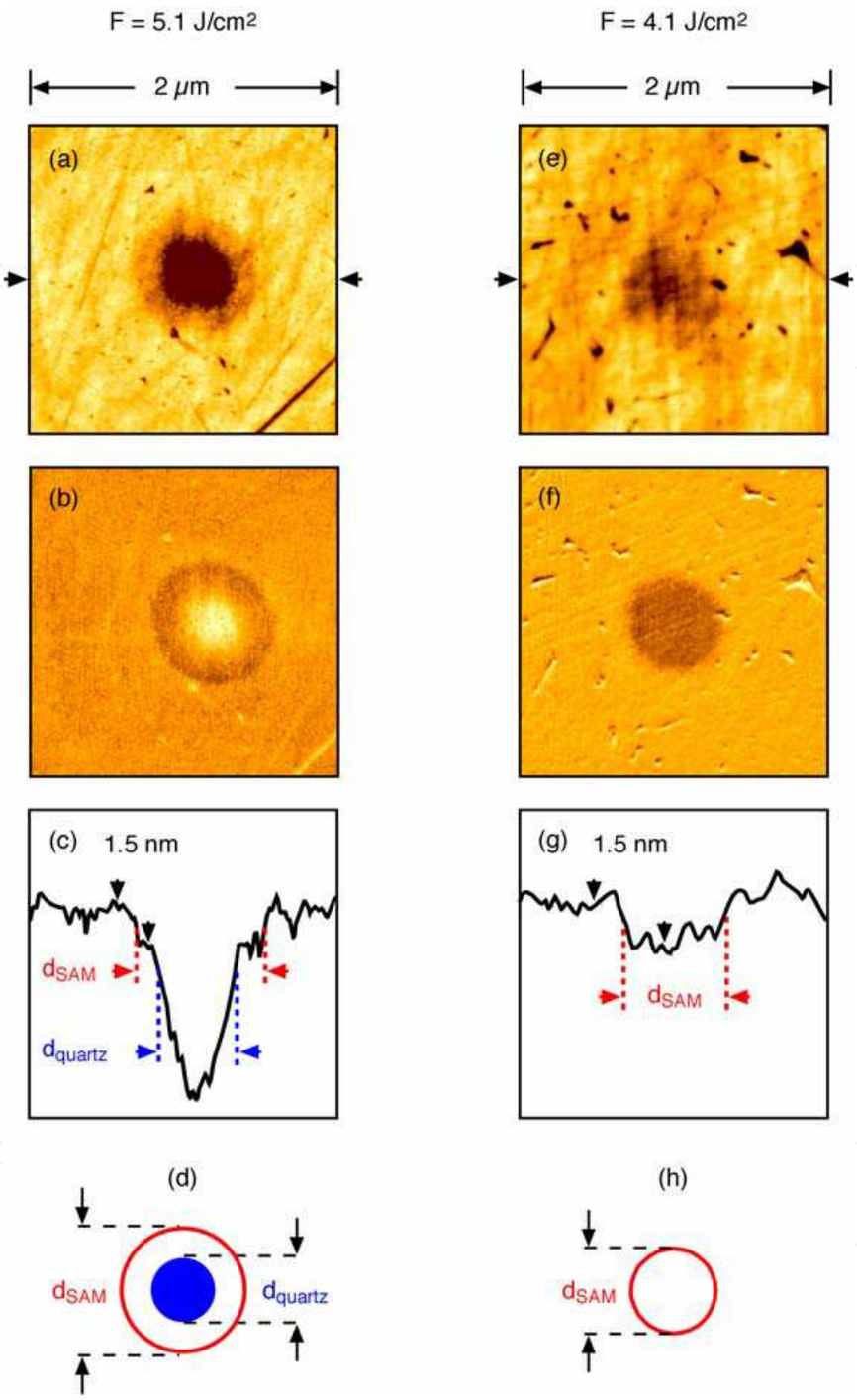

Fig. 4. AFM data from patterning experiments of ODS monolayers on quartz glass with single laser pulses at λ = 800 nm, τ < 30 fs and distinct fluences F: a) - d) F = 5.1 J/cm² and e) - h) F = 4.1 J/cm². The data display: a) and e) the topography, b) and f) the friction contrast, c) and g) height profiles. d) and h) are schematic presentations denoting the diameters d_{SAM} and d_{quartz}, where monolayer decomposition and substrate ablation are observed, respectively. Adapted from Hartmann et al., 2008. © AIP.

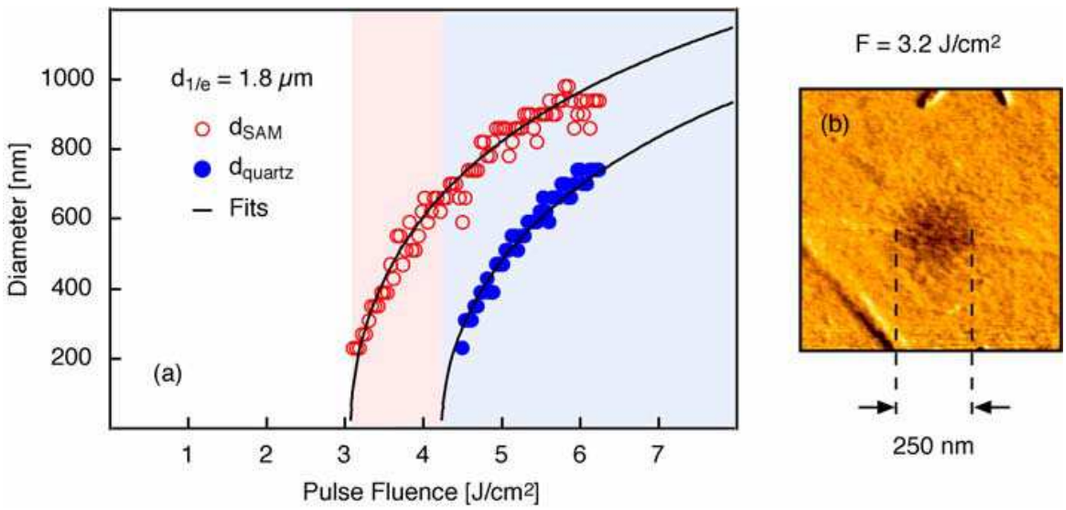

Fig. 5. AFM data from patterning experiments of ODS monolayers on quartz glass with single laser pulses at λ = 800 nm, τ < 30 fs: a) dependence of the diameters d_{SAM} and d_{quartz} on the laser pulse fluence. Lines are fits on the basis of Eq. (3). b) friction contrast image of a sub-wavelength structure at F = 3.2 J/cm². Adapted from Hartmann et al., 2008. © AIP.

This opens up an avenue towards laser fabrication of transparent templates with chemical structures down into the sub-100 nm regime. Such chemical templates represent promising platforms for biotechnological applications, e. g. DNA chips or other biosensor arrays. Processing at higher fluences, also provides a facile route towards combined chemical/topographic structures, e. g. for microfluidic applications. With these results and perspectives, quartz substrates represent an ideal platform for fs-laser processing of silane-based monolayers.

Noteworthy, only few techniques allow for direct nanopatterning of silane-based monolayers on dielectric substrates, such as quartz or glass. Photolithographic techniques, of course, can be used. Sub-100 nm patterning, e. g. using EUV lithography, though, remains challenging. Also, constructive techniques such as dip pen nanolithography and micro contact printing are complicated because of the intricate silane chemistry and surface charging impedes direct patterning with electron beam lithography.

3.2 Alkylsiloxane monolayers on surface-oxidized silicon

For comparison, fs-laser patterning experiments with alkylsiloxane monolayers on surface-oxidized silicon substrates are carried out (Franzka et al., 2010). With a linear photodissociation threshold E_D of 6 eV and a band gap E_B of 9 eV, both the organic monolayer and the surface silicon oxide film are highly transparent in the near-infrared regime. In contrast to quartz glass, however, the band gap of silicon is E_B = 1.1 eV. Hence, at a photon energy of E_P = 1.6 eV laser absorption essentially takes place in the silicon substrate. Monolayer decomposition appears possible via indirect processes. At sufficiently high fluences, multiple electronic excitations could to take place. In addition, photothermal pathways could open up even at comparatively low fluences. All these processes introduce strong nonlinearities and hence provide a means for patterning with sub-wavelength resolution.

AFM images from single-pulse patterning experiments at distinct fluences are shown in Fig. 6a. In contrast to the experiments with coated quartz glass substrates, local irradiation

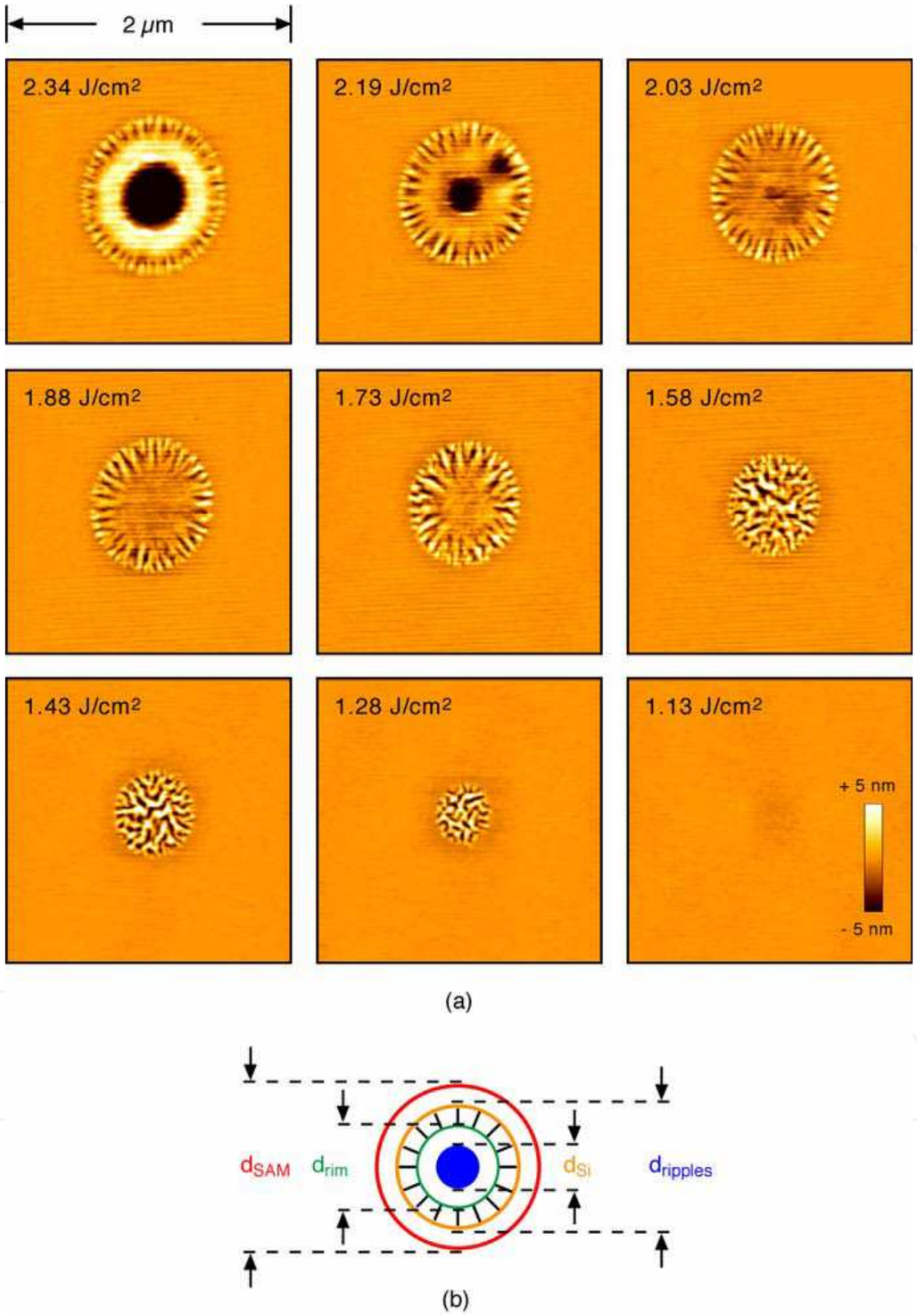

Fig. 6. a) AFM data from patterning experiments of ODS monolayers on surface-oxidized silicon substrates with single laser pulses at λ = 800 nm, τ < 30 fs and distinct fluences as indicated in the frames. b) schematic presentation depicting the diameters d_{SAM}, $d_{ripples}$, d_{rim} and d_{Si}. Adapted from Franzka et al., 2010. © AIP.

here results in a particularly rich complexity of surface morphology. At high fluences, at least four regions can be distinguished. In the centre region ablation of the substrate is evident (region 1). Radially outwards follow concentric areas where rim and ripples formation is observed (region 2 and 3, respectively) and a faint boundary area (region 4). If the fluence is reduced more and more, at first the depth of the hole in the centre decreases and the rim structure flattens. Finally, the inner regions disappear one after another and only a faint surface spot remains visible where monolayer decomposition has set in. In the following the diameters of the four regions are depicted as d_{Si}, d_{rim}, $d_{ripples}$ and d_{SAM}, respectively (Fig. 6b). In Fig. 7a a plot of these diameters over the laser fluence is displayed.

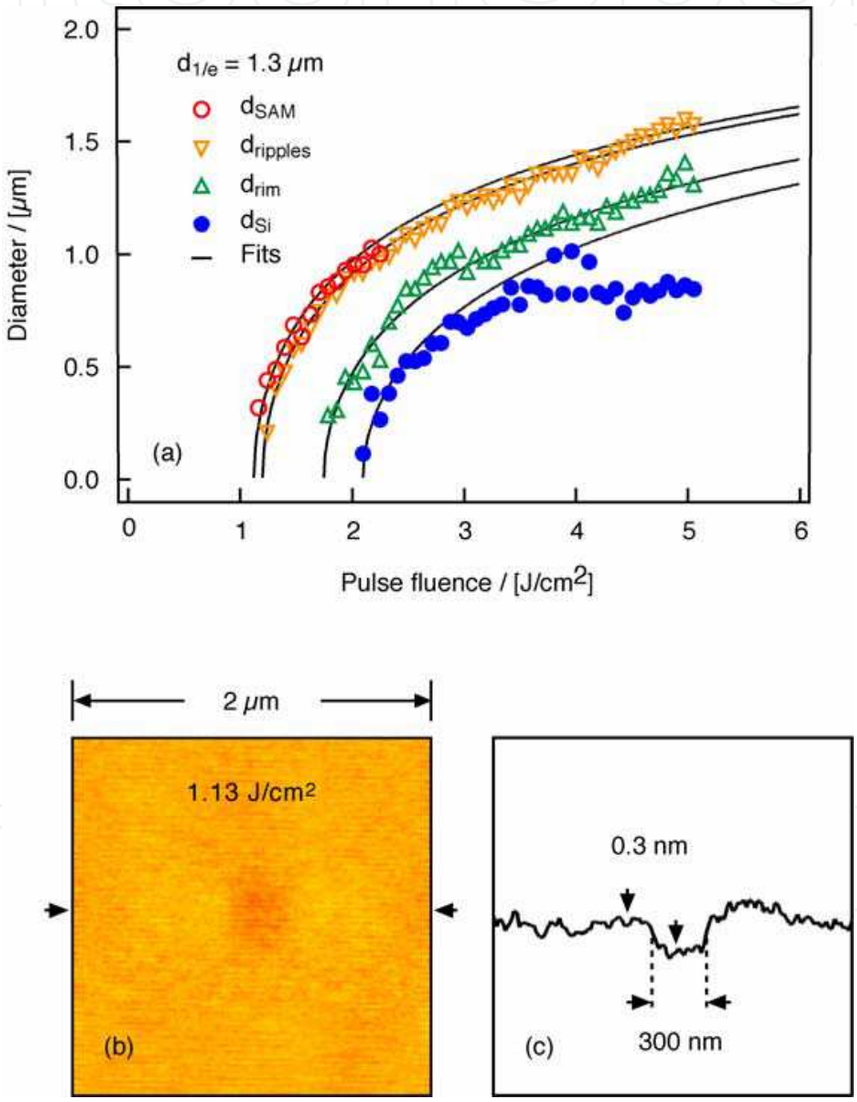

Fig. 7. AFM data from patterning experiments of ODS monolayers on surface-oxidized silicon substrates with single laser pulses at λ = 800 nm, τ < 30 fs: a) dependence of the diameters d_{hole}, d_{rim}, $d_{ripples}$ and d_{SAM} on the laser pulse fluence. Lines are fits on the basis of Eq. (3). b) and c) sub-wavelength structure at F = 1.13 J/cm²: b) topography and c) height profile across the structure in Fig. 7b. Adapted from Franzka et al., 2010. © AIP.

Noteworthy, despite a 1/e laser spot diameter of $d_{1/e}$ = 1.3 μm, minimum structure sizes for selective processing of the organic monolayer are about 300 nm. In particular, sub-wavelength patterning close to λ/3 is feasible. As shown in Figs. 7b and 7c, however, height profiles reveal depths of only 0.3 nm, that is, monolayer decomposition is largely incomplete. Moreover, the parameter range for selective fs-laser processing of alkylsiloxane monolayers on surface-oxidized silicon substrates is fairly narrow. Corresponding fits on the basis of Eq. (3) yield critical thresholds for substrate ablation, rim and ripples formation, and monolayer decomposition of F_{th}^{Si} = 2.1 J/cm², F_{th}^{rim} = 1.8 J/cm², $F_{th}^{ripples}$ = 1.2 J/cm² and F_{th}^{SAM} = 1.1 J/cm², respectively.

Alkylsiloxane monolayers, of course, exhibit an exceptional high thermal and photochemical stability (Onclin et al., 2005). Selective fs-laser processing of more sensitive organosiloxane monolayers is expected to be feasible in a significantly larger parameter range. Monolayers with tailored chromophors, here, are particularly promising (Onclin et al., 2005). In a recent contribution by Jonas, Kreiter and coworkers, for example, fs-laser patterning of silane-based SAMs with photoprotected carboxylic ester functionalities has been addressed (Álvarez et al. 2008). In addition, fs-laser processing of organic monolayers on oxide-free silicon appears promising (Buriak et al., 2002; Klingebiel; 2010). In particular, the Si/SiO_2 interface exhibits a valence band offset of around 4 eV. Hence in case of surface-oxidized samples, excited electrons in the substrate need higher energies in order to reach the organic coating on the surface. This could well block reactions, e. g. via multiple electronic excitations. SAMs on oxide-free silicon, in turn, are directly coupled to the semiconducting substrate and hence, generally, are more sensitive.

3.3 Alkanethiol monolayers on Au-coated silicon

If the fabrication of chemical templates is targeted, selective processing of the monolayers is a key requirement, e. g. in order to ensure precise vertical alignment of nanoscopic building blocks in subsequent deposition processes (Mathieu & Hartmann, 2010). SAMs, in turn, are also used as ultrathin resists. Generally, this makes lower demands on the selectivity of the process. In this respect, alkanthiol SAMs have been demonstrated to provide particularly promising perspectives in fs-laser processing as shown in Fig. 8 (Mathieu et al., 2010).

Similar to alkylsiloxane monolayers, alkanthiol monolayers are highly transparent at λ = 800 nm. Photochemical patterning of such SAMs usually is carried out at wavelengths in the deep ultraviolet range (Ryan et al., 2004). The linear photodissociation threshold E_D is close to 5 eV. At E_P = 1.6 eV, Au, in turn, exhibits a 1/e penetration depths of 14 nm. Hence, fs-laser processing of alkanthiol monolayers is expected to proceed via indirect mechanisms, which start with respective excitations in the substrate (cf. section 3.2).

Figs. 8a-c shows typical AFM images and corresponding height profiles from single-pulse patterning experiment at high fluences. As evident from this data, circular structures with two regions can be distinguished. In the outer region decomposition of the monolayer takes place. In particular, depths are 1-2 nm equivalent to the thickness of HDT SAMs on Au. In the inner region the formation of a fine tip structure indicative for substrate melting is visible (Koch et al.; 2005b). In agreement with these results, both regions exhibit a distinct friction contrast in comparison to the surrounding areas. Note, melting structures as those in Fig. 8a, of course, are undesirable when the fabrication of chemical templates is addressed. At lower fluences, melting structures are not observed anymore. The parameter window, for selective monolayer processing, though, is rather narrow. The melting structures, in turn, do

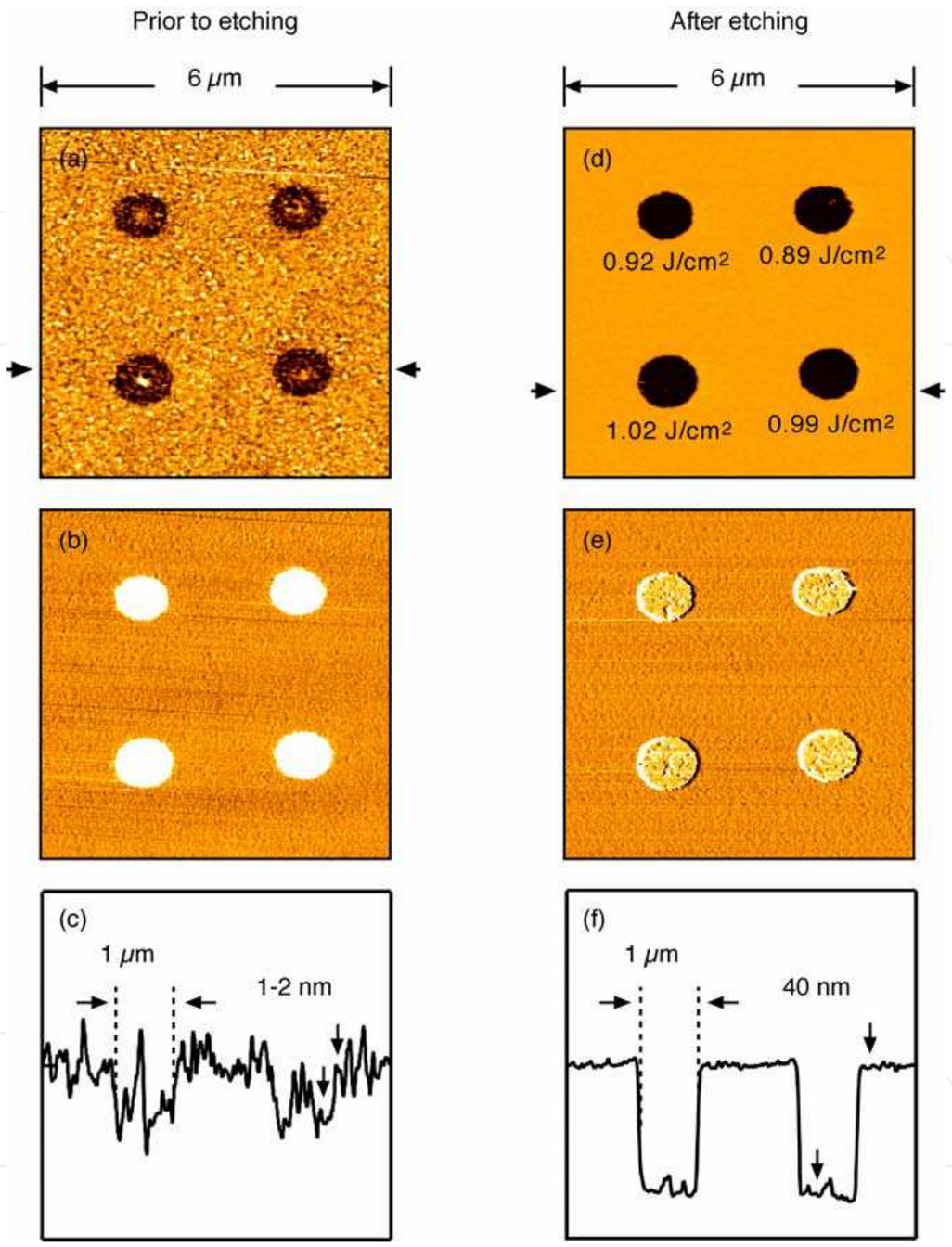

Fig. 8. AFM data from patterning experiments of HDT SAMs on Au-coated silicon samples with single laser pulses at λ = 800 nm, τ < 30 fs. a)-c) and d)-e) show the same surface area prior to etching and after etching in ferri-/ferrocyanide solution, respectively. Fluences at the distinct positions as indicated in d) are F = 0.89 J/cm², F = 0.92 J/cm², F = 0.99 J/cm² and F = 1.02 J/cm². a) and d) show the topography, b) and e) the friction contrast and c) and f) display height profiles at the positions marked by black arrows in a) and b). Black arrows in c) and f) indicate the width and the depth of the structures prior to etching and after etching, respectively. Adapted from Mathieu et al., 2010. © Springer.

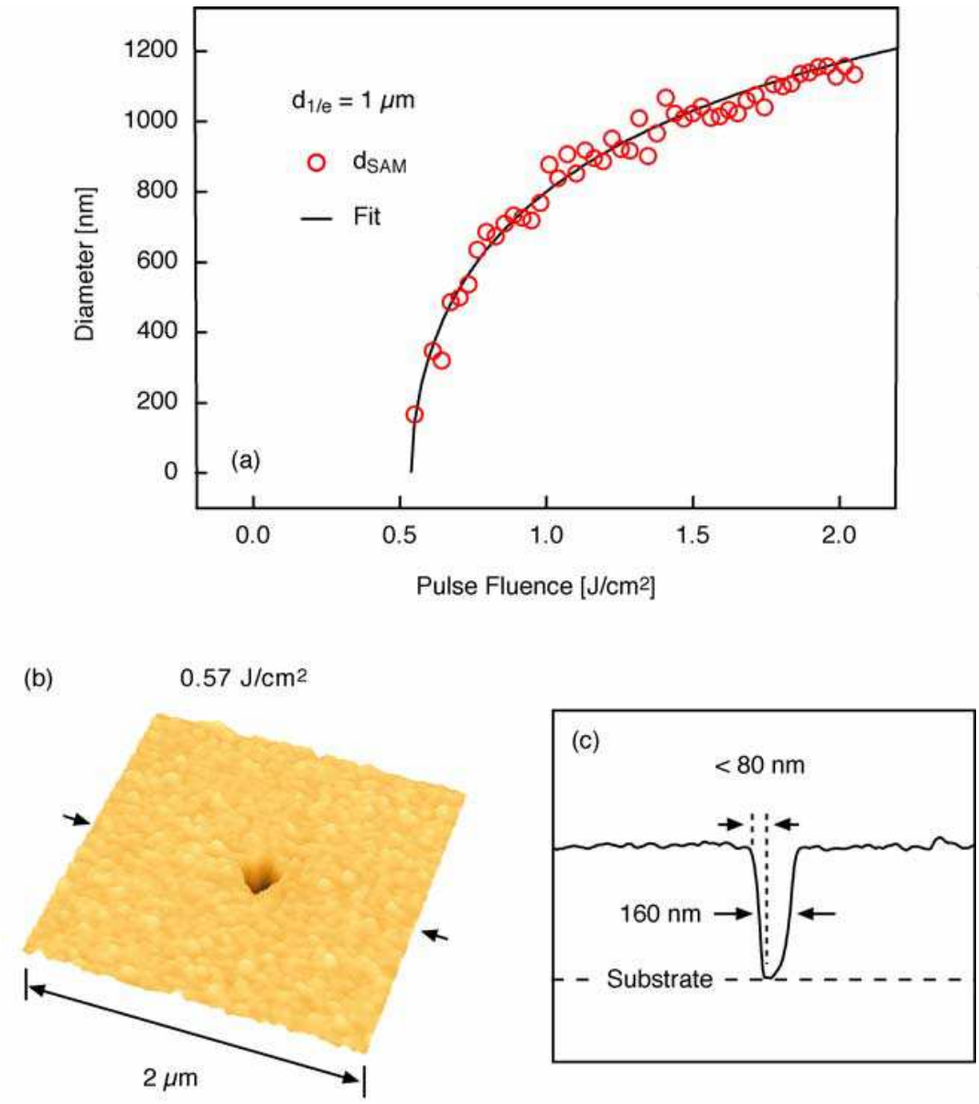

Fig. 9. AFM data from patterning experiments of HDT monolayers on Au-coated silicon substrates with single laser pulses at λ = 800 nm, τ < 30 fs: a) dependence of the diameters d_{SAM} on the laser pulse fluence. The line is a fit on the basis of Eq. (3). b) and c) sub-wavelength structure at F = 0.57 J/cm². b) shows the topography and c) displays a height profile across the structure in Fig. 9b. Adapted from Mathieu et al., 2010. © Springer.

not affect subsequent etching steps. Figs. 8d-f, for example, display the same structures as in Figs. 8a-c after etching in a ferri-/ferrocyanide solution (Xia et al., 1995). In the course of this process the 40 nm thick Au film in the bare surface areas is completely dissolved, whereas the SAM in the surrounding areas represents an effective resist layer. Hence, in this way the patterns are transferred into the Au film. No difference in etching is observed between the outer and inner region that are present after laser processing. This results in an extremely large processing window for pattern transfer.

From AFM height profiles the diameters of the etched structures at half-depth are obtained. As evident from Fig. 8, these diameters essentially correspond to the diameters d_{SAM} where

monolayer decomposition is initiated. In Fig. 9a a plot of d_{SAM} over the laser fluence is displayed. A fit on the basis of Eq. (3) yields a critical threshold for monolayer decomposition F_{th}^{SAM} = 0.53 J/cm². As expected from the observations discussed above, this value is close to the ablation threshold for thin Au films F_{th}^{Au} = 0.55 J/cm² reported in the literature (Kirkwood et al., 2007). Despite a 1/e spot diameter of $d_{1/e}$ = 1 μm, however, minimum structure sizes after pattern transfer are 160 nm. In particular, sub-wavelength patterning down to λ/5 is feasible. Respective AFM data are shown in Figs. 9b and 9c. Noteworthy, the full width of the step edge of these structures is 80 nm. This value is not corrected for tip size effects, that is, the actual width is expected to be even smaller. Altogether, these results demonstrate the prospects of alkanthiol monolayers as high-resolution resists in rapid nonlinear fs-laser processing.

4. Summary, conclusions and future perspectives

In conclusion, recent progress in single-pulse fs-laser processing of organic monolayers is reviewed. Processing with a micrometer-sized laser spot at λ = 800 nm and τ < 30 fs allows for sub-wavelength patterning. Generally, though, processing strongly depends on the particular chemical and electronic structure of the SAM/substrate system (Hartmann et al., 2008; Franzka et al., 2010; Mathieu et al., 2010). Tab. 1 summarizes the results discussed here. Processing of alkylsiloxane monolayers on quartz glass allows one to exploit multiphoton absorption processes (Hartmann et al., 2008). Selective patterning can be carried out in a fairly large range of laser pulse fluences with sub-wavelength resolution of λ/3 and below. This provides promising perspectives in fabrication of nanostructured chemical templates on transparent platforms, e. g. for biotechnological and microfluidic applications. Processing of alkylsiloxane monolayers on surface-oxidized silicon substrates is expected to follow an indirect mechanism, e. g. via multiple electronic excitations or photothermally induced reactions (Franzka et al., 2010). In contrast to the experiments on coated quartz samples, the parameter range for selective processing of alkylsiloxane monolayers on surface-oxidized silicon substrates is very narrow only. Moreover, monolayer decomposition here is largely incomplete. Hence, more sensitive monolayers are desired in order to exploit this approach on silicon substrates. In addition, fs-laser processing of organic monolayers on oxide-free silicon appears promising (Klingebiel; 2010). Similarly to alkylsiloxane monolayers on surface-oxidized silicon, processing of alkanethiol monolayers on Au-coated silicon is expected to proceed via indirect mechanims. The parameter range for selective processing, again, is rather narrow only. These SAMs, however, show great promise as high-resolution resists in rapid fs-laser processing of thin Au films. In particular, via etching the patterns can be transfered into the Au film. Minimum structures exhibit a width of λ/5.

Overall, these results demonstrate the general versatility of fs-lasers in nonlinear processing of SAMs on dielectric, semiconducting and metallic platforms. Considering tighter focusing optics and shorter wavelength sub-100-nm patterning appears feasible. In addition to its high lateral resolution, the procedure provides a powerful combination of other features, i.e., it is based on a noncontact maskless process and allows for rapid large-area patterning at ambient conditions.

Multiple-pulse patterning experiments also show that incubation effects generally are negligible warranting precise fabrication of complex patterns. In view of these results and

perspectives, fs-laser processing constitutes a powerful tool for large-area micro- and nanopatterning of self-assembled organic monolayers.

SAM / Substrate	E_D	E_B	$d_{1/e}$	d_{min}	λ/n	Critical Thresholds F_{th}	Processing window
ODS on quartz	6 eV	9 eV	1.8 µm	250 nm	$< \lambda/3$	F_{th}^{SAM} = 3.1 J/cm² F_{th}^{quartz} = 4.2 J/cm²	Patterning: 3.1 - 4.2 J/cm²
ODS on SiO_2/Si	6 eV	1.1 eV	1.3 µm	300 nm	$\approx \lambda/3$	F_{th}^{SAM} = 1.1 J/cm² $F_{th}^{ripples}$ = 1.2 J/cm² F_{th}^{rim} = 1.8 J/cm² F_{th}^{Si} = 2.1 J/cm²	Patterning: 1.1 – 1.2 J/cm²
HDT on Au/Si	5 eV	-	1.0 µm	160 nm	$\lambda/5$	F_{th}^{SAM} = 0.53 J/cm² F_{th}^{Au} = 0.55 J/cm²	Patterning: 0.53 – 0.55 J/cm² Pattern Transfer: 1.1 – 2.0 J/cm²

Tab. 1. Summary of the experimental results on fs-laser processing of organic monolayers with single laser pulses at λ = 800 nm, equivalent to E_P = 1.6 eV, τ < 30 fs. For focusing, optics with NA = 0.5 are used (Hartmann et al., 2008; Franzka et al., 2010; Mathieu et al., 2010).

On a broader view, the results reported here nicely complement previous studies focusing on sub-wavelength patterning of SAMs via nonlinear processing with continuous-wave lasers exploiting photothermal processes (Balgar et al., 2006; Dahlhaus et al., 2006; Mathieu et al., 2009; Klingebiel et al., 2010; Mathieu & Hartmann, 2010).

5. Acknowledgements

Financial support by the Deutsche Forschungsgemeinschaft (DFG, Grant HA-2769/3-1), the BASF Coatings GmbH and the European Union and the Ministry of Economic Affairs and Energy of the State North Rhine-Westphalia in Germany (NanoEnergieTechnikZentrum, NETZ, Objective 2 Programme: European Regional Development Fund, ERDF) is gratefully acknowledged. It is a pleasure to thank my coworkers and collaborators, who contributed to the work presented here: Steffen Franzka and Mareike Mathieu at the University of Duisburg-Essen, Andreas Ostendorf at the Ruhr University Bochum and Jürgen Koch and Boris Chichkov at the Laser Zentrum Hannover, where all laser experiments have been carried out. I'm also grateful to Eckart Hasselbrink for his continuing support.

6. References

Ali, M .; Wagner, T.; Shakoor, M. & Molian, P.A. (2008). Review of laser nanomachining, J. Laser Appl., Vol. 20, pp. 169-184.

Álvarez, M.; Best, A.; Pradhan-Kadam, S.; Koynov, K.; Jonas, U. & Kreiter, M. (2008). Single-photon and two-photon induced photocleavage for monolayers of an

alkyltriethoxysilane with a photoprotected carboxylic ester, Adv. Mater., Vol. 20, pp. 4563-4567.

Balgar, T.; Franzka, S.; Hartmann, N. (2006). Laser-assisted decomposition of alkylsiloxane monolayers at ambient conditions: rapid patterning below the diffraction limit, Appl. Phys. A, Vol. 82, pp. 689-695.

Bäuerle, D. (2000). Laser processing and chemistry, Springer, Berlin.

Buriak, J.M. (2002). Organometallic chemistry on silicon and germanium surfaces, Chem. Rev., Vol. 102, pp 1271–1308.

Chang, W.; Choi, M.; Kim, J.; Cho, S. & Whang, K. (2005). Sub-micron scale patterning using femtosecond laser and self-assembled monolayers interaction, Appl. Surf. Sci., Vol. 240, pp. 296-304.

Chang, W.; Kim, J.; Cho, S. & Whang, K. (2006). Femtosecond-laser-coupled near-field scanning optical microscopy patterning using self-assembled monolayers, Jpn. J. Appl. Phys., Vol. 45, pp. 2082-2086

Chong, T.C.; Hong, M.H. & Shi, L.P. (2010). Laser precision engineering: from microfabrication to nanoprocessing, Laser and Photonics Rev., Vol. 4, pp 123-143.

Dahlhaus, D.; Franzka, S.; Hasselbrink, E.; Hartmann, N. (2006). 1D nanofabrication with a micrometer-sized laser spot, Nano Letters, Vol. 6, pp. 2358-2361.

Franzka, S.; Koch, J.; Chichkov, B.N. & Hartmann, N. (2010). Nonlinear femtosecond laser processing of alkylsiloxane monolayers on surface-oxidized silicon substrates, J. Vac. Sci. Technol. A, Vol. 28, pp. 814-817.

Hartmann, N.; Franzka, S.; Koch, J.; Ostendorf, A. & Chichkov, B.N. (2008). Subwavelength patterning of alkylsiloxane monolayers via nonlinear processing with single femtosecond laser pulses, Appl. Phys. Lett., Vol. 92, pp. 223111-1-223111-3.

Kirkwood, S.E.; Shadnam, M.R.; Amirfazli, A. & Fedosejevs, R. (2007). Mechanism for femtosecond laser pulse patterning of self-assembled monolayers on gold- coated substrates, J. Phys.: Conf. Ser., Vol. 59, pp. 428-431.

Klingebiel, B.; Scheres, L.; Franzka, S.; Zuilhof, H. & Hartmann, N. (2010). Photothermal micro- and nanopatterning of organic/silicon interfaces, Langmuir, Vol. 26, pp. 6826-6831.

Koch, J.; Fadeeva, E.; Engelbrecht, M.; Ruffert, C.; Gatzen, H.H.; Ostendorf, A. & Chichkov, B.N. (2006). Maskless nonlinear lithography with femtosecond laser pulses, Appl. Phys. A, Vol. 82, pp. 23-26.

Koch, J.; Korte, F.; Fallnich, C.; Ostendorf, A. & Chichkov, B.N. (2005a), Direct-write sub-wavelength structuring with femtosecond laser pulses, Opt. Eng., Vol. 44, pp. 051103-1-051103-5.

Koch, J.; Korte, F.; Bauer, T.; Fallnich, C.; Ostendorf, A. & Chichkov, B.N. (2005b), Nanotexturing of gold films by femtosecond laser-induced melt dynamics, Appl. Phys. A, Vol. 81, pp. 325-328.

Love, J.C.; Estroff, L.A.; Kriebel, J.K.; Nuzzo, R.G. & Whitesides, G.M. (2005). Self-assembled monolayers of thiolates on metals as a form of nanotechnology, Chem. Rev., Vol. 105, pp. 1103-1170.

Mathieu, M.; Franzka, S.; Koch, J.; Chickov, B.N. & Hartmann, N. (2010). Self-assembled organic monolayers as high-resolution resists in rapid nonlinear processing with single femtosecond laser pulses, Appl. Phys. A, Vol. 101, pp. 461-466.

Mathieu, M. & Hartmann, N. (2010). New J. Phys., in press

Mathieu, M.; Schunk, D.; Franzka, S.; Mayer, C.; Hasselbrink, E.; Hartmann, N. (2009), Direct laser patterning of soft matter: photothermal processing of supported phospholipid multilayers with nanoscale precision, Small, Vol. 5, pp. 2099-2104.

Onclin, S.; Ravoo, B.J. & Reinhoudt, D.N. (2005). Engineering silicon oxide surfaces using self-assembled monolayers, Angew. Chem. Int. Ed., Vol. 44, pp. 6282-6304.

Richter, L.J. & Cavanagh, R.R. (1992). Mechanistic studies of photoinduced reactions at semiconductor surfaces, Prog. Surf. Sci., Vol. 39, pp. 155-226.

Ryan, D.; Parviz, B.A.; Linder, V.; Semetey, V.; Sia, S.K.; Su, J.; Mrksich, M. & Whitesides, G.M. (2004). Patterning multiple aligned self-assembled monolayers using light, Langmuir, Vol. 20, pp. 9080-9088.

Sugimura, H.; Ushiyama, K.; Hozumi, A. & Takai, O. (2000). Micropatterning of alkyl- and fluoroalkylsilane self-assembled monolayers using vacuum ultraviolet light, Langmuir, Vol. 16, pp. 885-888.

Woodson, M. & Liu, J. (2007). Functional nanostructures from surface chemistry patterning, Phys. Chem. Chem. Phys., Vol. 9, pp. 207-225.

Xia, Y.; Zhao, X.M.; Kim, E. & Whitesides, G.M. (1995). A selective etching solution for use with patterned self-assembled monolayers of alkanethiolates on gold, Chem. Mater., Vol. 7, pp. 2332-2337.

Zhou, X.L.; Zhu, X.Y. & White, J.M. (1991). Photochemistry at adsorbate/metal interfaces, Surf. Sci. Rep., Vol. 13, pp. 73-220.

Zimmermann, F.M. & Ho, W. (1995). State resolved studies of photochemical dynamics at surfaces, Surf. Sci. Rep., Vol. 22, pp. 127-247.

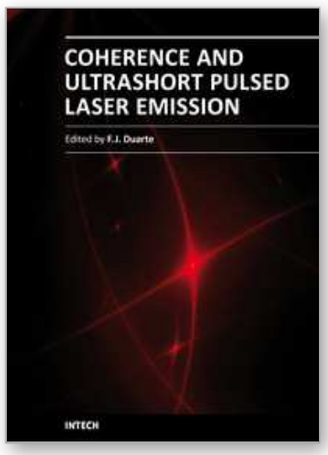

Coherence and Ultrashort Pulse Laser Emission
Edited by Dr. F. J. Duarte

ISBN 978-953-307-242-5
Hard cover, 688 pages
Publisher InTech
Published online 30, November, 2010
Published in print edition November, 2010

In this volume, recent contributions on coherence provide a useful perspective on the diversity of various coherent sources of emission and coherent related phenomena of current interest. These papers provide a preamble for a larger collection of contributions on ultrashort pulse laser generation and ultrashort pulse laser phenomena. Papers on ultrashort pulse phenomena include works on few cycle pulses, high-power generation, propagation in various media, to various applications of current interest. Undoubtedly, Coherence and Ultrashort Pulse Emission offers a rich and practical perspective on this rapidly evolving field.

INTECH
open science | open minds

InTech Europe
University Campus STeP Ri
Slavka Krautzeka 83/A
51000 Rijeka, Croatia
Phone: +385 (51) 770 447
Fax: +385 (51) 686 166
www.intechopen.com

InTech China
Unit 405, Office Block, Hotel Equatorial Shanghai
No.65, Yan An Road (West), Shanghai, 200040, China
中国上海市延安西路65号上海国际贵都大饭店办公楼405单元
Phone: +86-21-62489820
Fax: +86-21-62489821

IntechOpen